Vibration Control of Parallel Platforms based on Magnetorheological Damping

Memet Unsal, Carl D. Crane, III
University of Florida
Dept. of Mechanical & Aerospace Engineering
Gainesville, FL 32611
+1 352 392-9461
memetu@ufl.edu

Christopher Niezrecki
University of Massachusetts Lowell
Dept. of Mechanical Engineering
Lowell, MA 01854
+1 978 934-2963
Christopher_Niezrecki@uml.edu

ABSTRACT
Within this work a model of a 6 DOF (degree-of-freedom) vibration isolation system with semi-active control, using magnetorheological (MR) technology is investigated. The geometry of the parallel platform is determined in a way which maximizes the Quality Index. Parallel platform mechanisms are ideal candidates for 6 DOF positioning and vibration isolation. A 6 DOF parallel platform which utilizes semi-active vibration control has not received as much attention as its passive and active counterparts have. The advantages of semi-active control include reduced cost by using a simpler actuator intended for only positioning, reduced power requirements, and improved stability. Within this work, the legs of a parallel platform model are investigated by implementing a two DOF Simulink model. Each leg of the platform is modeled as a two DOF system with a magnetorheological (MR) damper for adjustable damping.

Keywords
Parallel platform, magnetorheological, semi-active, vibration control, hexapod.

1. INTRODUCTION
Parallel platform mechanisms have received a lot of attention due to their distinct advantages over their serial counterparts. They have six serial kinematic chains (connectors) giving them greater load carrying capacity, higher stiffness, and redundancy in motion which make them more tolerant to individual actuator positioning errors [1]. These advantages make them ideal for precision positioning applications. However, many of these applications are located in environments where certain degrees of disturbances exist. These disturbances in the form of vibrations degrade the performance of the sensitive instruments which are essential for precision positioning. Therefore, it is important to create a vibration-free environment to enable precision positioning. From a design perspective, it would be logical to have a hexapod which is inherently an ideal mechanism for precise positioning to provide vibration isolation at the same time.

Structures and mechanical systems should be designed to enable better performance under different types of loading, particularly dynamic and transient loads. There are three fundamental control strategies to regulate or control the response of a system: passive control, active control, and semi-active control. The performance of a passive system is limited because system parameters such as damping cannot be varied. Active control can change the properties of the system based on the change in the instantaneous operating conditions as measured by sensors [2]. However, besides requiring a significant external power supply for actuators, active control has the inherent danger of becoming unstable through the injection of mechanical energy into the system. Semi-active control has been developed as a compromise between passive and active control. A semi-active control system is incapable of injecting energy into a system, but can achieve favorable results through selective energy dissipation [3]. Instead of directly opposing a primary disturbance, semi-active vibration control is used to apply a secondary force, which counteracts the effects of the disturbance by altering the properties of the system, such as stiffness and damping [4]. The adjustment of mechanical properties, which is based on feedback from the excitation and/or from the measured response, is what differentiates semi-active control from passive control. A controller monitors the feedback measurements and an appropriate command signal is generated for the semi-active devices. Unlike an active system, the control forces developed are generated by the motion of the structure. Furthermore, the stability of the semi-active system is guaranteed as the control forces typically oppose the motion of the structure and can only remove energy from the system [5]. In principle, a semi-active damper can emulate an active system as long as the required control force input of the active system is used to dissipate energy and the supply of energy into the system is not required. While active and passive vibration control have been extensively used in parallel platforms, a 6 DOF parallel platform which utilizes semi-active vibration control has not received as much attention.

The robustness and the simple mechanical design of magnetorheological (MR) dampers make them a natural candidate for a semi-active control device. They require minimal power while delivering high forces suitable for full scale applications. They are fail-safe since they behave as passive devices in case of a power loss [6]. MR fluids are suspensions of small iron particles in a base fluid. They are able to reversibly change from free-flowing, linear viscous liquids to semi-solids having controllable yield strength under a magnetic field. When the fluid is exposed to a magnetic field, the particles form linear chains parallel to the applied field as shown in Figure 1. These chains impede the flow and solidify the fluid in a matter of milliseconds.

This phenomenon develops a yield stress which increases as the magnitude of the applied magnetic field increases [7].

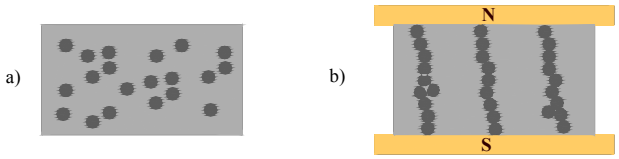

Figure 1. Magnetorheological fluid: a) no magnetic field, b) with magnetic field

2. THEORETICAL BACKGROUND

2.1 Magnetorheological (MR) Damper Design

MR devices can be divided into three groups of operational modes, valve mode, direct shear mode, and squeeze mode or a combination of the three based on the design of the device components. In the valve mode, of the two surfaces that are in contact with the MR fluid, one surface moves relative to the fluid. This relative motion creates a shear stress in the fluid. The shear strength of the fluid may be varied by applying different levels of magnetic field. In the direct shear mode, the fluid is pressurized to flow between two surfaces which are stationary. The flow rate and the pressure of the fluid may be adjusted by varying the magnetic field. In the squeeze film mode, two parallel surfaces squeeze the fluid and the motion of the fluid is perpendicular to that of the surfaces. The applied magnetic field determines the force needed to squeeze the fluid and also the speed of the parallel surfaces during the squeezing motion [7].

The magnetic circuit typically uses low carbon steel, which has a high magnetic permeability and saturation. This steel effectively directs magnetic flux into the fluid gap. Several different designs of MR dampers have been built and tested in the past. The first of these designs is the bypass damper where the bypass flow occurs outside the cylinder and an electromagnet applies a magnetic field to the bypass duct [8,9]. A simple schematic of this damper is displayed in Figure 2a. While this design has a clear advantage that the MR fluid is not directly affected by the heat build-up in the electromagnet, the presence of the bypass duct makes it a less compact design. Figure 2b shows the schematic of a design by the Lord Corporation, where the electromagnet is inside the cylinder and the MR fluid passes through an annular gap between the electromagnet and the inner cylinder. This design uses an accumulator to make up for the volume of fluid displaced by the piston rod which is going into the damper [10,11]. The design in Figure 2b can be modified to have two shafts so that the accumulator which compensated for the volume of fluid displaced by the shaft going into the damper is no longer necessary. The outer housing is made up of low carbon steel. Therefore the flux lines pass through the housing in their return path while the magnetorheological fluid flows through the annular gap between the housing and the magnetic body around which the coil is wound as seen in Figure 3. The magnetic body is designed to divide the coil into two parts which creates three effective magnetic surfaces. The two coils are wound in directions opposite to each other so that the flux lines add up in the middle.

There are several different models in the literature used to characterize the behavior of MR dampers. The most common is the Bingham plastic model which is also the one that is used in this work. This model is an extension of the Newtonian flow and it is obtained by also taking into account the yield stress of the fluid. It assumes that flow will occur when the dynamic yield stress is reached. The total stress is given by

$$\tau = \tau_y \,\mathrm{sgn}(\dot{\gamma}) + \eta\dot{\gamma} \tag{1}$$

where τ_y is the yield stress induced by the magnetic field, $\dot{\gamma}$ is the shear rate and η is the viscosity of the fluid. In this model, the relationship between the damper force and the shear velocity may also be given as

$$F = \begin{Bmatrix} F_y \,\mathrm{sgn}(\dot{x}) + C_o\dot{x} & \dot{x}\neq 0 \\ -F_y < F < F_y & \dot{x}=0 \end{Bmatrix} \tag{2}$$

where C_o is the post-yield damping coefficient and F_y is the yield force. In the post-yield part, the slope of the force-velocity curve is equal to the damping coefficient which is essentially the viscosity of the fluid, η. Both C_o and F_y are functions of the control current input, i and can be modeled as second order polynomial functions:

$$\begin{aligned} F_y(i) &= F_{yc}i^2 + F_{yb}i + F_{ya} \\ C_o(i) &= C_c i^2 + C_b i + C_a \end{aligned} \tag{3}$$

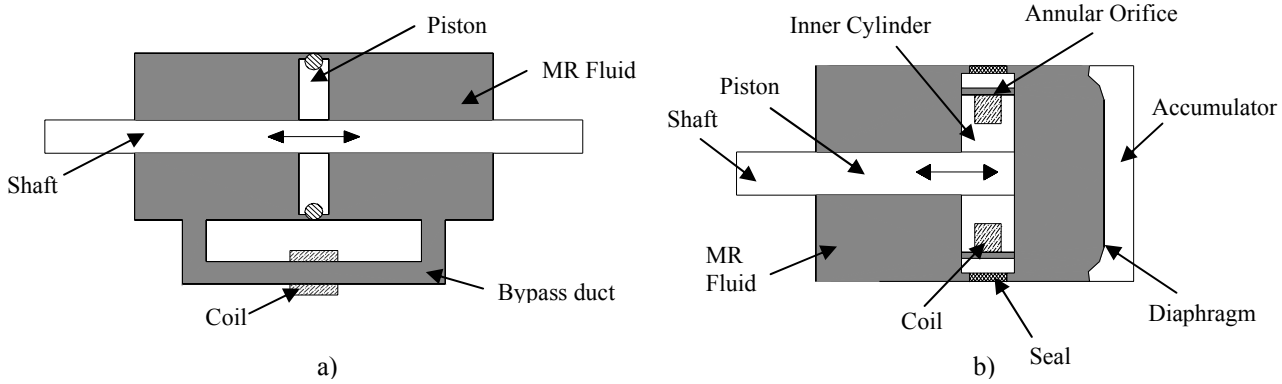

Figure 2. a) Schematic of the by-pass type MR damper b) Schematic of RD-1500

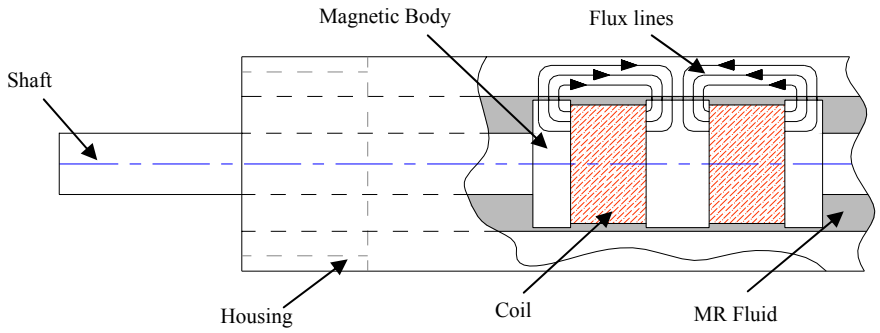

Figure 3. Schematic of the double-shafted MR damper

The model coefficients may be found by minimizing the mean square error between the experimental and the model-predicted damper force. The values used in this work were experimentally calculated by Ni et al. and are as follows [12]

$$F_y(i) = -39.8i^2 + 95.1i + 21.0$$
$$C_o(i) = 25.6i^2 + 376i + 220 \quad (4)$$

Other MR damper fluid models in the literature include the Herschel-Bulkley model which takes into account the post-yield shear thinning and thickening behavior and the Bouc-Wen model where the parameters of the model can be adjusted to control the linearity in the unloading and the smoothness of the transition from the pre-yield to the post-yield region [11].

2.2 Vibration Control

Consider the case of the single-axis passive isolator where m is the mass of sensitive equipment, k and c are the stiffness and damping of the isolator respectively. Figure 4 shows that when the damping ratio is increased, the resonance that appears at the natural frequency decreases, but the sharpness of the roll-off at high frequency decreases too. When the damping ratio is equal to 0, the high frequency roll-off is $1/s^2$ (40 dB/decade) while very large amplitude is seen near the natural frequency. On the other hand, when the damping ratio is increased, we reduce the response at the resonance, but we also reduce the roll-off to 1/s (-20 dB/decade) [13,14]. As a result, the design of a passive damper involves a trade-off between the resonance and high frequency attenuation.

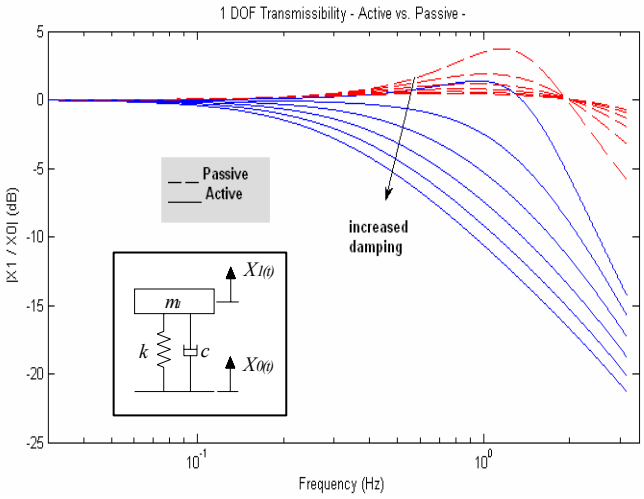

Figure 4. Transmissibility between X_1 and X_0 of the single DOF mass-spring-damper system with passive and active skyhook damper control (m_1 = 85 kg, k = 16,000 N/m, c = 700, 1200, 1700, 2200, 2700, 3200 Ns/m)

The resonance at the natural frequency may be avoided without the penalty of reduced high frequency isolation by using the "skyhook damper" control. It is called skyhook damper control because the active control force is proportional to the clean body absolute velocity as if the clean body were connected to an inertial frame [15]. Figure 4 shows that in the active control, the increase in the damping coefficient reduces the resonance at the natural frequency and the high frequency decay rate does not suffer either. Similar results are shown in Figure 5 for the two DOF model.

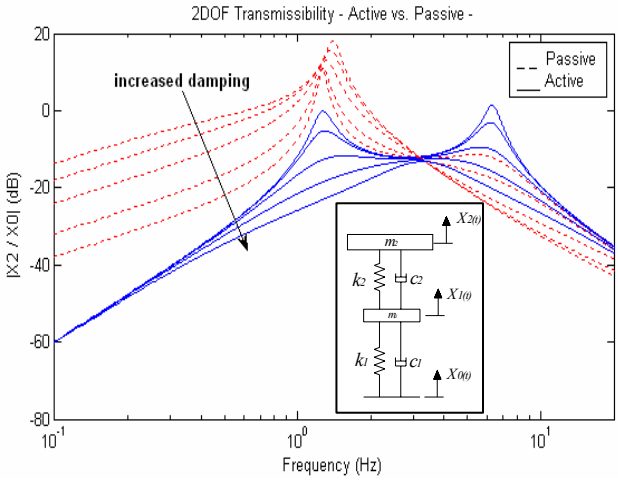

Figure 5. Transmissibility of the two DOF mass-spring-damper system with passive and active skyhook damper control (m_1 = 5 kg, k_1 = 2,000 N/m, c_1 = 10 Ns/m, m_2 = 20 kg, k_2 = 5,000 N/m, c_2 = 100, 200, 500, 1000, 1700 Ns/m)

The semi-active damper can only dissipate energy, so in the semi-active implementation of the skyhook damper control an input current to the damper is only applied when the relative velocity between the two bodies and the absolute velocity of the clean body are in the same direction. Otherwise, the damping coefficient is set to its minimum value which is when the input current is equal to 0. The control policy is therefore

$$F = \begin{cases} F_{\max} & \text{when} \quad (\dot{x}_2 - \dot{x}_1)\dot{x}_2 > 0 \\ F_{\min} & \text{when} \quad (\dot{x}_2 - \dot{x}_1)\dot{x}_2 \le 0 \end{cases} \quad (5)$$

2.3 Parallel Platform Model

It is a difficult task for a designer to determine the geometry of a parallel platform mechanism due to the complexity of its kinematics. Its behavior is not as intuitive as a serial manipulator and the geometric properties which will cause singularities are difficult to identify [20,21]. The quality index was proposed to facilitate the design process of the parallel platform mechanism.

It was initially defined for a planar 3-3 parallel mechanism [22] and later extended to the 6-6 parallel mechanism [23] which is the geometry examined within this work. It is defined by the dimensionless ratio

$$\lambda = \frac{|\det \boldsymbol{J}|}{|\det \boldsymbol{J}|_{\max}} \tag{6}$$

where $\boldsymbol{J}$ is the six-by-six matrix of the normalized coordinates of the six leg lines and $|\det \boldsymbol{J}|_{\max}$ is the greatest absolute value of the determinant of this Jacobian matrix. The quality index takes a maximum value of 1 at the central configuration. When the top platform departs from the central configuration, the determinant of the Jacobian matrix always diminishes and it is zero when a singularity is encountered where the platform gains one or more uncontrollable freedoms. Therefore, $0 \le \lambda \le 1$ at every reachable configuration. The quality index is dependent neither on the choice of units of the leg lengths nor on the coordinate frame in which the line coordinates are determined. It is dependent solely on the configuration [24].

Within this work, the quality index is used to determine the relative sizes of the base and the top platform and the initial height of the top platform. Not only were designs which would lead to low or zero quality indexes avoided, but also the geometry of the 6-6 parallel platform was determined by setting dimensions which gave the highest quality index possible.

The geometry of the top platform and the base platform are displayed in Figure 6. Both platforms are an equilateral triangle with the tips of the triangle removed where the joints are located. The joints are separated symmetrically by an angle of 2.5 degrees on each side of the internal angle bisector which passes through the orthocenter of the triangle. This corresponds to a distance of αa between each two top platform joint where $\alpha = 0.047$ and a distance of βb between each two base platform joint where $\beta = 0.047$.

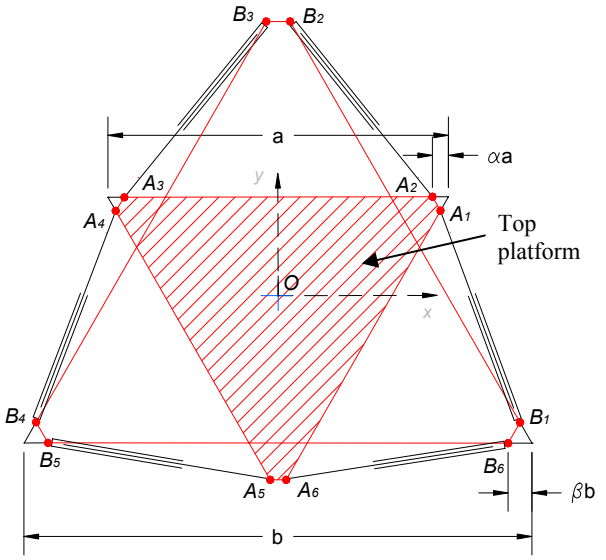

Figure 6. 6-6 Parallel platform schematic showing the orientation of top platform to base platform

Figure 6 shows the orientation of the top platform to the bottom platform where the top is rotated 60 degrees from the bottom. The top platform is raised to a distance of h and the top is connected to the bottom through the six legs A_1B_1, A_2B_2, A_3B_3, A_4B_4, A_5B_5, and A_6B_6.

The normalized determinant of the six leg lines is

$$\det \boldsymbol{J} = \frac{1}{l^6}\left|\boldsymbol{S}^{\mathrm{T}}{}_1 \quad \boldsymbol{S}^{\mathrm{T}}{}_2 \quad \boldsymbol{S}^{\mathrm{T}}{}_3 \quad \boldsymbol{S}^{\mathrm{T}}{}_4 \quad \boldsymbol{S}^{\mathrm{T}}{}_5 \quad \boldsymbol{S}^{\mathrm{T}}{}_6\right| \tag{7}$$

where $l = B_1A_1 = B_2A_2 = B_3A_3 = B_4A_4 = B_5A_5 = B_6A_6$ is the same length for each leg. The derivative of the determinant is taken to find the height of the top platform and the ratio of the size of the base platform to the size of the top platform which maximize the determinant. The geometry of the 6-6 parallel platform model used in the simulations are based on this optimal configuration.

3. SIMULATIONS

The MR damper was modeled in Simulink according to the Bingham plastic model and the model parameters are given in Equation (4). The input to the model is the relative velocity between the two masses (m_1 and m_2 in Figure 7) which the damper connects and the control current. In the simulations, the MR damper is assumed to respond very fast and the time delay associated with the damper's response time is ignored.

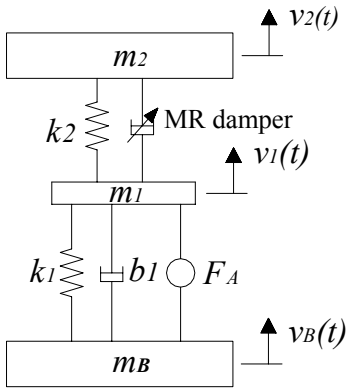

Figure 7. Two DOF platform leg model with MR damper

The MR damper is implemented in a two DOF leg model. The connector leg consists of an actuator in series with the MR damper-spring pair. The stiffness and the friction of the actuator are modeled as a spring-damper pair in parallel with a force element as shown in Figure 7.

The two DOF leg system model has the Bingham plastic model MR damper and an on/off control algorithm. In this algorithm, the MR damper is either turned on by applying a 2A input current or it is turned off by setting the input current to 0A. No intermediate current is applied. The bottom mass (m_B) is subjected to a sinusoidal disturbance and the transmissibility between the top (m_2) and the bottom mass is calculated.

In Figure 8, constant input currents are applied to the MR damper in a single DOF system as uncontrolled cases to be compared. It is seen that the displacement of the sprung mass is reduced by

utilizing the on/off control. Also, the power requirement for the controlled system would be less than having a 2A input current applied to the MR damper continuously.

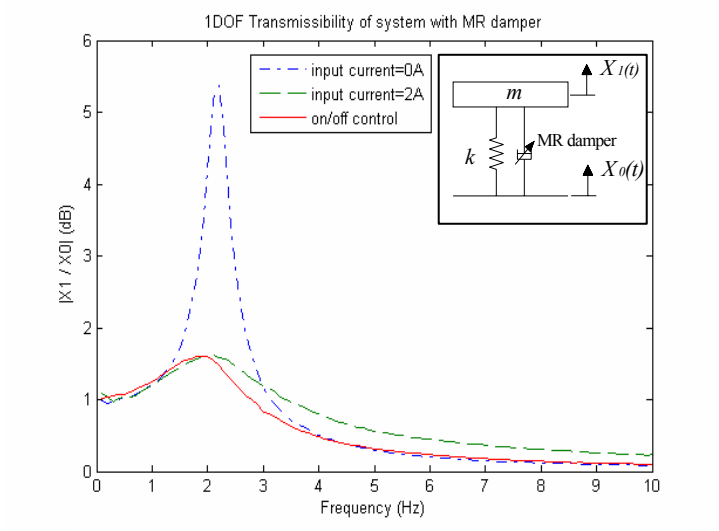

Figure 8. Transmissibility of the single DOF mass-spring-MR damper system with 0A input current, 2A input current, and on/off control (m = 85 kg, k = 16,000 N/m)

Figure 9 shows the transmissibility between the displacement of the top mass and the input excitation of a two DOF system. This model forms the basis of the connector legs of the six DOF platform system. The first mass, m_1, is the upper leg which would include the mass of the actuator piston and the MR damper. The second mass, m_2, is the portion of the parallel manipulator's top platform mass that a single leg has to carry. In this model, when a continuous 2A input current is applied to the MR damper, the link between the first mass, m_1, and the second mass, m_2, behaves almost as a rigid element. This is why the transmissibility is high for the first frequency, and the second peak is missing. On/off control reduces the peak at the first frequency and provides a lower transmissibility at higher frequencies.

The two DOF model previously described forms the basis of the connector legs of the six DOF platform system. The six DOF parallel platform mechanism was also modeled in SimMechanics. The bottom platform of the mechanism is subjected to a sinusoidal excitation and the transmissibility of the top platform is calculated. A drawing of the modeled parallel platform mechanism is shown in Figure 10. Implementation and response results of the 6 DOF model will be presented in a future publication.

4. CONCLUSIONS AND FUTURE WORK

A six DOF parallel platform mechanism was modeled in SimMechanics. Each leg of the platform is a two DOF model with an MR damper for adjustable damping. In the simulations, it was shown that active skyhook damper control can reduce the transmissibility between the top mass and the bottom mass of the connector leg much better than passive control for a two DOF model. An on/off control was implemented for the semi-active MR damper to replace the active control system. The future work will focus on extending the two DOF simulations with the semi-active system to the six DOF parallel platform mechanism. The response of the top platform of the parallel platform mechanism will be observed when the bottom platform is subjected to a disturbance. The performance of the semi-active control system with the MR damper will be compared to the performance of the active skyhook damper control.

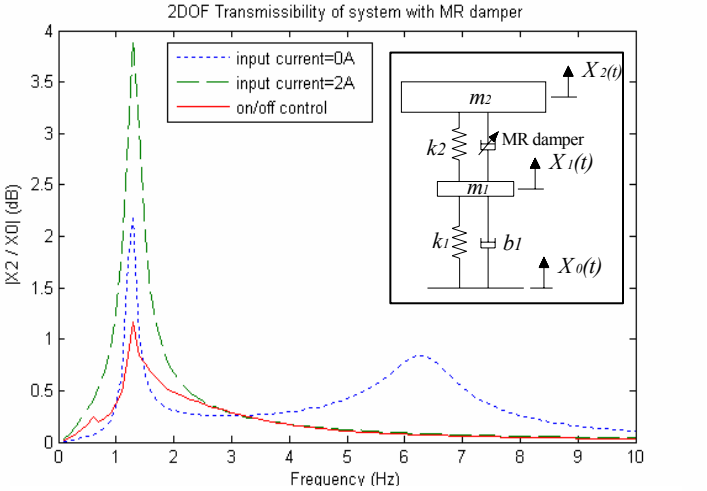

Figure 9. Transmissibility of the two DOF mass-spring-MR damper system with 0A input current, 2A input current, and on/off control (m_1=5 kg, k_1=2000 N/m, b_1=10 Ns/m, m_2=20 kg, k_2=5000 N/m)

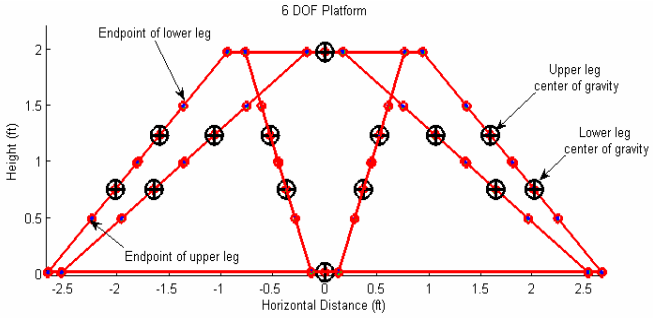

Figure 10. Six DOF parallel platform mechanism

5. REFERENCES

[1] Anderson, E. H., Cash, M. F., Hall, J. L., and Pettit, G. W., Hexapods for precision motion and vibration control. *American Society for Precision Engineering, Control of Precision Systems*, (April 2004).

[2] Hac, A. and Youn, I., Optimal semi-active suspension with preview based on a quarter car model. *J Vib Acoust Stress Reliab Des*, 114, 1 (Jan 1992), 84-92.

[3] Scruggs, J. and Lindner, D., Active energy control in civil structures. In *Proceedings of SPIE - The International Society for Optical Engineering*, 3671 (1999) 194-205.

[4] Brennan, M. J., Day, M. J., and Randall, R. J., Experimental investigation into the semi-active and active control of longitudinal vibrations in a large tie-rod structure. *Journal of*

Vibration and Acoustics, Transactions of the ASME, 120, 1 (Jan 1998), 1-12.

[5] M.D. Symans and M.C. Constantinou, Experimental testing and analytical modeling of semi-active fluid dampers for seismic protection. *Journal of Intelligent Material Systems and Structures*, 8, 8, (Aug. 1997), 644-657.

[6] Jolly, M. R., Bender, J. W., and Carlson, J. D., Properties and applications of commercial magnetorheological fluids. In *Proceedings of SPIE - The International Society for Optical Engineering*, 3327 (1998) 262-275.

[7] Yalcintas, M., Magnetorheological fluid based torque transmission clutches. In *Proceedings of the International Offshore and Polar Engineering Conference*, 4 (1999), 563-569.

[8] Sodeyama, H., Sunakoda, K., Fujitani, H., Soda, S., Iwata, N., and Hata, K., Dynamic tests and simulation of magneto-rheological dampers. *Computer-Aided Civil and Infrastructure Engineering*, 18, 1 (Jan. 2003), 45-57.

[9] Sunakoda, K., Sodeyama, H., Iwata, N., Fujitani, H., and Soda, S., Dynamic characteristics of magneto-rheological fluid damper. In *Proceedings of SPIE - The International Society for Optical Engineering*, 3989, (2000), 194-203.

[10] Snyder, R. A., Kamath, G. M., and Wereley, N. M., Characterization and analysis of magnetorheological damper behavior due to sinusoidal loading. In *Proceedings of SPIE - The International Society for Optical Engineering*, 3989, (2000), 213-229.

[11] Snyder, R. A. and Wereley, N. M., Characterization of a magnetorheological fluid damper using a quasi-steady model. In *Proceedings of SPIE - The International Society for Optical Engineering*, 3668, I, (1999), 507-519.

[12] Ni, Y. Q., Liu, H. J., and Ko, J. M., Experimental investigation on seismic response control of adjacent buildings using semi-active MR dampers. *Smart Structures and Materials 2002: Smart Systems for Bridges, Structures, and Highways*, 4696, (2002), 334-344.

[13] Collins, S. A. and von Flotow, A. H., Active vibration isolation for spacecraft. *42nd Congress of the International Astronautical Federation*, 289, (Montreal, Canada, 1991).

[14] Rivin, E. I., Principles and criteria of vibration isolation of machinery. *ASME, Trans. of the Journal of Mechanical Engineering*, 101, (1979), 682–692.

[15] A. Preumont, *Vibration Control of Active Structures: An Introduction*, Kluwer Academic Publishing, Boston, (2002), 116-119.

[16] Fichter, E. F., A Stewart Platform-Based Manipulator: General Theory and Practical Construction. *The International Journal of Robotics Research*, 5, (1986), 157-182.

[17] Merlet, J. P., Singular Configurations of Parallel Manipulators and Grassmann Geometry. *The International Journal of Robotics Research*, 8, 5, (1989), 45-56.

[18] Lee, J., Duffy, J., and Keler, M., The Optimum Quality Index for the Stability of In-Parallel Planar Platform Devices. In *Proceedings of the ASME 24th Biennial Mechanisms Conference, 96-DETC/MECH-1135*, (Irvine, CA, 1996).

[19] Lee, J., and Duffy, J., The Optimum Quality Index for Some Spatial In-Parallel Devices. *Florida Conference on Recent Advances in Robotics*, (Gainesville, FL, April 1999).

[20] Lee, J., *Investigations of Quality Indices of In-Parallel Platform Manipulators and Development of Web Based Analysis Tool*, Ph.D. thesis, University of Florida, Gainesville, FL, 2000.